Molecular Dynamics Simulations of Multicomponent Diffusion. 2. Nonequilibrium Method

Dean R. Wheeler* and John Newman

Department of Chemical Engineering, University of California, Berkeley, Berkeley, California 94720

Received: May 18, 2004; In Final Form: September 1, 2004

We describe a new nonequilibrium molecular dynamics algorithm for simulating multicomponent diffusion within the Stefan−Maxwell framework. The approach developed here allows for the efficient computation of a full diffusion-coefficient matrix for solutions containing any number of species. Due to our interest in electrolytes, the method is tested by simulating aqueous KCl and NaCl salt solutions in the concentration range 1−4 *m*. The results are in semiquantitative agreement with experiment and in quantitative agreement with previous Green−Kubo calculations for our potential models. This provides strong evidence that the equilibrium and nonequilibrium methods are correct.

1. Introduction

In this paper (part 2) and a preceding companion paper (part 1),[1] we successfully demonstrate that molecular dynamics (MD) can be used to calculate all of the relevant mass-transport coefficients for isothermal solutions having an arbitrary number of components. This paper will describe the development and validation of a nonequilibrium method for calculating diffusivities, a method that is complementary to the equilibrium Green−Kubo method developed in paper 1.

Nonequilibrium molecular dynamics (NEMD) methods are perhaps the most intuitive way to obtain transport properties, because of these methods' similarity to physical experiments. NEMD algorithms have been designed to obtain a whole range of transport properties. In each of these NEMD algorithms, the simulated system is perturbed away from equilibrium and the subsequent response of the system is measured. The perturbation can be either transient or steady-state; it can be implemented as an external field, as a boundary condition, or as a nonuniform initial condition. The response, generally a flux of some conserved variable, can be obtained easily since all particle positions and momenta are known in the simulation. To connect the perturbation to the response, an assumption is made that linear transport laws apply to this microscopic system. In this way a transport property can be calculated, and by assumption corresponds to the same property generated by a macroscopic experiment.

In this paper, we outline the currently used NEMD algorithms for mass transport, discussing both advantages and drawbacks to each. We show that one of these, field-driven NEMD, is the best choice for our work on liquid electrolytes. Finally, we describe how field-driven NEMD can be adapted to obtain all of the independent bulk-diffusion coefficients for an arbitrary number of species, a procedure that is new to this work.

As in paper 1, we refer specificially to the calculation of bulk- or collective-diffusion coefficients, as opposed to the self- or tracer-diffusion coefficients commonly calculated in molecular dynamics studies found in the literature. The oft perceived equivalence of tracer diffusion and bulk diffusion is only justified for highly dilute solutes.

* To whom correspondence should be addressed. Present address: Department of Chemical Engineering, Brigham Young University, Provo, UT 84602. E-mail: dean_wheeler@byu.edu.

Our linear constitutive equation for describing multicomponent diffusion is a form of the Stefan−Maxwell equation[2]

$$c_a \nabla \mu_a = \sum_{b \neq a} K_{ab}(\mathbf{v}_b - \mathbf{v}_a) \tag{1}$$

where the a and b subscripts cover the n species. c is molar concentration, μ is electrochemical potential, and $\mathbf{v}$ is the species velocity vector. K_{ab} is a "friction" coefficient between species a and b and can be related to a "binary interaction" diffusion coefficient $\mathscr{D}_{ab}$. With the appropriate substitutions more fully described in paper 1, eq 1 can be inverted to read

$$\mathbf{J}_a = \sum_{b \neq 0} L^0_{ab} \mathbf{X}_b \tag{2}$$

where $\mathbf{J}_a = \mathbf{v}_a - \mathbf{v}_0$ and $\mathbf{X}_a = -c_a \nabla \mu_a$. In the inversion process the solvent is assigned as species 0. In this framework μ is termed the electrochemical potential to indicate that both concentration gradients and electric potential fields can be used to drive species fluxes. However, at this stage we do not consider the thermodynamic factors, Γ_{ab}, which in practice are required to get driving force $\mathbf{X}_a$ in terms of concentration gradients. Matrix $\mathbf{L}^0$ has dimensions $(n-1) \times (n-1)$, is symmetric, and contains all the linear mass-transport information for an isothermal n-component system; that is, other mass-transport-coefficient representations may be uniquely determined from $\mathbf{L}^0$.[2]

2. NEMD Algorithms

As we alluded above, there are several different NEMD diffusion algorithms that have been used to obtain mass-transport properties. The algorithms can be categorized by the method of perturbation used to drive species flux. In this section we describe the two main types found in the literature.

Boundary-Driven (Inhomogeneous) NEMD. Several NEMD algorithms (indeed, the first ones ever tried) rely on spatial inhomogeneity to drive transport. For diffusion simulations this inhomogeneity is a variation in species concentration across the simulation cell.[3] To maintain a steady-state concentration profile, mass must be injected on one side of the cell, and removed from the other side of the cell; hence the term "boundary-driven" NEMD.

10.1021/jp047849c CCC: $27.50 © 2004 American Chemical Society
Published on Web 11/02/2004

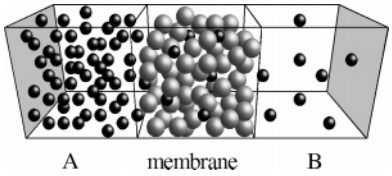

Figure 1. Representation of a dual-control-volume grand-canonical molecular dynamics simulation. The smaller spheres constitute species 1, the diffusing species; the larger spheres constitute species 2, the membrane.

Boundary-driven algorithms generally use a simulation cell that is periodic in two dimensions. The nonperiodic dimension is the one in which diffusion takes place. Figure 1 illustrates a type of simulation developed concurrently by MacElroy[4] and by Heffelfinger and co-workers.[5] The algorithm is now known as dual-control-volume grand-canonical molecular dynamics (DCV-GCMD). The simulation cell is divided into three regions: control volume A (CVA), a membrane, and control volume B (CVB). A chemical-potential (i.e., concentration) difference of species 1 is maintained between CVA and CVB. This leads to a steady-state flux of species 1 through the membrane region. Particles of species 2 are confined to the membrane region and comprise the membrane. To maintain the chemical-potential difference, particles of species 1 must be inserted into CVA and deleted from CVB, hence the "grand-canonical" part of the algorithm name.

The DCV-GCMD method has been used and refined by a few research groups.[6−9] With current computer hardware, the method is suitable for simulating membranes that have a thickness on the order of 1−5 nm. However, the method has serious limitations for our purposes. The use of continuous and long-range potentials, as opposed to short-range potentials such as hard-sphere or truncated Lennard-Jones potentials, makes it difficult to perform the particle insertions and deletions without disturbing the dynamics. To get a suitable response from the system, the concentration gradient in the membrane must be quite steep, and it becomes difficult to obtain diffusivities as a function of concentration. The Maginn group also discovered that, under the action of large fluxes, there is significant interphase resistance: particles of species 1 must arrange themselves in order to leave CVA and enter the pores of the membrane. Because of the small thickness of the membrane, it is difficult to separate bulk membrane behavior from this interphase resistance.[9]

A wholly different inhomogeneous NEMD technique, based on the use of initial conditions, was developed by Maginn et al.[10] In this technique, called gradient-relaxation molecular dynamics, species 1 is initially given a sawtooth concentration profile within a stationary matrix of species 2. This inhomogeneity is allowed to relax over the course of the simulation, leading to a mutual diffusion coefficient through application of the diffusion equation (Fick's second law). This technique suffers from the difficulty of obtaining adequate sampling (due to the lack of a steady state) and the requirement of large initial concentration differences. It does not appear to have been pursued in any subsequent works.

Field-Driven (Homogeneous) NEMD. In field-driven or homogeneous NEMD, an external field is applied to the simulation cell. The field couples to some particle property, such as charge or mass, and exerts a body force on the particles. In response, the particles undergo a net movement or flux that is, in the isotropic case, parallel or antiparallel with the field vector.

The first homogeneous NEMD simulations of mass transport employed the so-called color-diffusion or color-current algorithm, developed by Denis Evans and co-workers.[11−14] *Color diffusion* means that the external field interacts with a fictitious color charge assigned to each particle. Half of the ensemble of particles has a color charge of +1, while the other half has a color charge of −1, resulting in mutual diffusion between the two color groups. Because particles of the two groups are otherwise chemically identical, the algorithm in effect generates a self-diffusion coefficient, which was found to compare well to the Green-Kubo value.

The natural evolution of the color-diffusion algorithm was to simulate mutual diffusion between two species. In this instance, the color charges are assigned according to the chemical identity of each molecule. All of the early work involved mutual diffusion in Lennard-Jones mixtures.[11,14] Lennard-Jones particles are good approximations to noble gases, and their liquid mixtures are fairly ideal, meaning that the thermodynamic factor Γ_{12} is nearly unity. This allowed direct comparison of the simulated $\mathscr{D}_{12}$ to experimental Fick's law D_{12}. Later NEMD work simulated species diffusion in polymers, lattices, and pores.[9,10,15]

An important point that came out of the color-diffusion work was that the imposed field need not be physically real, leading Evans and Morriss to characterize the field as *synthetic*.[13] In other words, one can choose an arbitrary body force to act on each molecule, so long as the total external force on the system is zero. The use of synthetic fields gives one tremendous flexibility in designing computer diffusion experiments. Because the forces on the species do not depend on position and periodic boundary conditions are employed, the simulation remains homogeneous, having no sustained concentration gradients.

The use of synthetic fields does not mean that the calculated diffusivities are unphysical. Beginning with the work of Nernst and of Einstein, it has been recognized that diffusion coefficients are functionally equivalent to mobilities, and mobilities should be independent of the particular force generating the species flux. Indeed, this idea of force equivalence is intrinsic to using a thermodynamic driving force: a given chemical-potential gradient can be generated by an unlimited number of different possible concentration gradients in a multicomponent solution. Moreover, the equivalence of electric potential fields, pressure gradients, and concentration gradients as driving forces is well established in the Stefan−Maxwell framework.[2,16] The equivalence has been successfully exploited in a number of separation schemes including centrifugal separation and electrophoresis. In experimental practice, there is a limited number of diffusional driving forces that can be employed; molecular simulations need not be similarly restricted.

As an aside, we postulate the microscopic basis for this driving-force equivalence as follows. In the linear-transport limit, all nonequilibrium driving forces are *small* perturbations about the fluctuating (equilibrium) intermolecular forces. Regardless of the exact physical nature of the perturbations, there is a universality to the way the molecules in a given system dynamically arrange themselves in order to dissipate the small perturbations. One can see this universality by recognizing that the equilibrium fluctuations, being essentially white noise, sample all possible small perturbations. The fluctuation−dissipation theorem[17] then allows us to connect the stochastic equilibrium fluctuations to a universal response function. This postulate means that any from a set of thermodynamically equivalent (not necessarily experimentally achievable) driving forces will lead to consistent species fluxes. The diffusion coefficients, so obtained, are thus insensitive to the physical basis of the driving forces.

In the most-used form of homogeneous NEMD, a constant external field is applied to the system, and the subsequent steady-state diffusional velocities of the species are measured. Another possibility for a homogeneous field-driven scheme is to allow the external field to vary with time. A number of schemes have been proposed including sinusoidal, step-change, and delta-function time-varying fields.[3,18] A possible advantage of these implementations is that they allow frequency-dependent transport properties to be obtained. The disadvantage, in practice, is that the lack of a steady state makes it difficult to thermostat the system properly and to obtain adequate sampling of zero-frequency properties. The time-varying-field approach is not used in the present work.

We believe that the best way to obtain transport properties for *bulk* solutions is constant-field-driven NEMD. The method's primary advantage is that the concentrations of the respective species are spatially and temporally constant during a given simulation. This allows the resulting mass-transport coefficients to be determined as a function of concentration. In addition, as a homogeneous method, field-driven NEMD minimizes finite-size effects on simulation results. Finally, we note the recent report from the Maginn group where field-driven NEMD was five times more computationally efficient than an inhomogeneous DCV-GCMD method.[9]

Handling Large Fields. One of the advantages of field-driven NEMD, relative to GK algorithms, is that the signal-to-noise ratio in the calculated transport coefficients can be made arbitrarily large simply by increasing the strength of the field. Unfortunately, this luxury is also a necessity. Due to the large computational expense of MD, only small sample sizes and times can be simulated with existing computer hardware. This means that obtaining reasonable signal-to-noise ratios requires that field strengths be several orders of magnitude greater than what is used generally in experiments.

An algorithm change is made in recognition of the fact that the fields employed in NEMD are so large, that is, a numerical "themostat" is required in order to achieve a steady-state response. This is due to the immense Joule- or Ohm-type heating that takes place under the action of species fluxes coupling to large external fields. A Nosé-Hoover thermostat[19,20] is used here, with a time constant that resulted in cell thermal fluctuations on a 100-fs time scale.

Unfortunately, the thermostat in turn creates a problem: it interacts with the net motion or flux of each species. The manifestation of this interaction, under large fields, is a free-energy advantage to partial phase separation of the system. Rather than remaining homogeneous, the system tends to form streaming phases or "finger instabilities", much like opposing lanes of traffic on a road.[11,12] This has the effect of reducing inter-species frictional contact, leading to anomalously large diffusivities.

The phase-separation artifact can be suppressed by a minor change to the coupling of the thermostat to particle momenta, a change originating with Evans and co-workers. This is reflected in the following equations of motion for particle i

$$\dot{\mathbf{r}}_i = \frac{\mathbf{p}_i}{m_i} \tag{3}$$

$$\dot{\mathbf{p}}_i = \mathbf{f}_i - \zeta(\mathbf{p}_i - m_a\mathbf{v}_a) + \mathbf{F}_a^{\mathrm{ex}} \tag{4}$$

where $\mathbf{r}_i$ is position and $\mathbf{p}_i$ is momentum for particle i, which is a member of species a. m_a is the mass of the particle, $\mathbf{v}_a$ is the instantaneous aggregate species velocity, and F_a^{ex} is the force on the particle due to the external field. In the present context, $\mathbf{F}_a^{\mathrm{ex}} = V\mathbf{X}_a/N_a$, where V is cell volume and N_a is the number of particles of species a. ζ is a relative heat removal or addition rate (units of time^{-1}) determined by a separate equation. Equations 3 and 4 do not include additional terms required to control the cell pressure.

If we sum the modified thermostat term in eq 4 over all particles i of species a, we get zero

$$\sum_{i\in a}\zeta(\mathbf{p}_i - m_a\mathbf{v}_a) = 0 \tag{5}$$

which ensures that the thermostat has no effect on the species flux. More elaborate corrections to the thermostat are possible[21] but appear to be unnecessary in the present context.

Even with this algorithm change, one cannot always escape noticeable (and physical) nonlinear responses in systems with large sustained field strengths. In 1927, Wien and Malsch announced that the conductivity of electrolytic solutions increases under the influence of large electric-potential gradients.[22] Now known as the Wien effect, this genuine nonlinearity can be observed in large-field simulations, as shown below. An analogous nonlinear behavior is observed in NEMD viscosity simulations, namely shear thinning of Newtonian fluids under the action of very large strain rates.

To conclude this section, we make a few additional comments on the synthetic fields used in our simulations. Many of our fields have a close physical analogue; however, there are differences. Our synthetic electric field acts only on the centers of mass of ions. This is in contrast to an actual electric field, which additionally exerts a torque on dipolar molecules or molecular segments. The other synthetic fields used here similarly act only on molecular centers of mass. In this sense, the synthetic fields most resemble a gravitational field. Although this simplification is not strictly necessary, it makes selection of synthetic fields easier. Our synthetic fields generate the essential property we need to measure, namely molecular translational motion.

Our simulations will not exhibit dielectric breakdown, which would be undesirable in this context. All Coulombic charges and covalent bonds in our molecular models are rigid and are not influenced by the external fields. While the synthetic electric fields we use can be large (up to 8×10^8 V/m), they are below the predicted level at which an electric field can dissociate and ionize bulk water, about 10^{11} V/m.[23] Our synthetic electric fields do, however, approach the levels found in the electric double layer adjacent to metal electrodes.[23]

3. Calculating Multicomponent Mass-Transport Coefficients

Many of the above principles of NEMD simulations are found in the literature; however, the adaptation of these ideas to multicomponent systems as done in this work is new. In this section, we describe our method for calculating Stefan−Maxwell mass-transport coefficients.

Experimental Approach. The method resembles an experimental approach to the problem, albeit with a greater degree of flexibility in the choice of driving forces used. That is, we impose driving forces, measure the resulting fluxes, and then regress the transport coefficients.

For mathematical compactness in describing the procedure, we make a few notational changes in this section. Isotropic transport is assumed, meaning that fluxes J_a and driving forces X_a always take place in the same direction. We now define the

vectors **X** and **J** as each being composed of $n - 1$ elements, one for each species $a = 1, \ldots, n - 1$ (species 0 is the solvent). Substituting this change into eq 2 gives a compact expression of the linear transport law

$$\mathbf{J} = \mathbf{L}^0\mathbf{X} \tag{6}$$

How many computer experiments do we need to run? There are $n(n - 1)/2$ independent coefficients in an isothermal n-component system. Each one-dimensional experiment yields a maximum of $n - 1$ independent pieces of information, namely the species fluxes **J**. Thus, one needs to conduct a minimum of $n/2$ independent experiments (rounding the number up to the next higher integer, of course). However, by *initially* neglecting Onsager's reciprocal relation (ORR), our regression procedure is made simpler. In this case there are temporarily $(n - 1)^2$ independent mass-transport coefficients, requiring at least $n - 1$ experiments to resolve.

Thus, we conduct a series of $\mathcal{N}_{\text{exp}}$ computer experiments, where $\mathcal{N}_{\text{exp}} \geq n - 1$. $\mathbf{X}^\gamma$ and $\langle\mathbf{J}\rangle^\gamma$ are respectively the driving forces and resulting average fluxes for experiment γ, where $\gamma = 1, \ldots, \mathcal{N}_{\text{exp}}$. To resolve $\mathbf{L}^0$, the set of $\mathbf{X}^\gamma$ must contain a subset of $n - 1$ mutually orthogonal vectors $\mathbf{X}^\gamma$. That is, there must be an adequate basis set to span the multicomponent-diffusion space. This is the meaning of the term "orthogonal experiments" as used by experimentalists.

Because of simulation uncertainties, we allow the possibility of performing a greater number of computer experiments than is absolutely necessary, to improve the quality of the regressed coefficients. For instance, one may want to repeat experiments over a range of field strengths and obtain a matrix $\mathbf{L}^0$ that best fits the data. The problem, then, is how to obtain a transport-coefficient matrix that satisfies, in a least-squares sense, as many experiments as we care to perform. The normal mathematical procedure to accomplish this is known as singular value decomposition and is generally cumbersome. However, we obtain a much simpler, and yet mathematically equivalent procedure as follows. First we write the mass-transport equation for a single experiment γ

$$\langle\mathbf{J}\rangle^\gamma = \mathbf{L}^0\mathbf{X}^\gamma \tag{7}$$

Next, we multiply by $\mathbf{X}^{\gamma\,\mathrm{T}}$ from the right, and sum over all experimental samples γ. Superscript T indicates the transpose operation, in this case changing a column vector into a row vector

$$\sum_\gamma \langle\mathbf{J}\rangle^\gamma \mathbf{X}^{\gamma\mathrm{T}} = \mathbf{L}^0 \sum_\gamma \mathbf{X}^\gamma \mathbf{X}^{\gamma\,\mathrm{T}} \tag{8}$$

The final step is to perform a matrix inversion

$$\mathbf{L}^0 = \left[\sum_\gamma \langle\mathbf{J}\rangle^\gamma \mathbf{X}^{\gamma\,\mathrm{T}}\right]\left[\sum_\gamma \mathbf{X}^\gamma \mathbf{X}^{\gamma\,\mathrm{T}}\right]^{-1} \tag{9}$$

Like other least-squares procedures, eq 9 can handle the limiting case where the number of independent samples equals the number of unknown parameters. The above procedure assumes that all random error lies in the "dependent" variable $\langle\mathbf{J}\rangle$, rather than the "independent" variable **X**. This will be the case when driving forces are fixed. If the set of $\mathbf{X}^\gamma$ is an inadequate basis, the matrix to be inverted in eq 9 will be singular. In two-component mixtures, the preceding work is made trivial, due to the reduction of all matrixes and vectors to scalars.

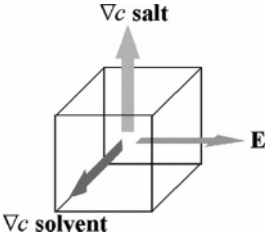

Figure 2. Representation of simultaneous orthogonal experiments conducted during one simulation.

As stated before, we do not initially enforce ORR. The built-in redundancy in the possibly asymmetric form of $\mathbf{L}^0$ (eq 9) ensures that we do not prematurely discard any information that contributes to the off-diagonal or cross-diffusional terms. Moreover, the degree of skewness in $\mathbf{L}^0$ can serve as a gauge of simulation uncertainties. The reciprocal relation is then enforced by letting $\mathbf{L}^0$ be the result of $(\mathbf{L}^0 + \mathbf{L}^{0\mathrm{T}})/2$. This is done before deriving other properties, such as conductivity, from $\mathbf{L}^0$.

Three-Fold Increase in Efficiency. Another advantage of field-driven NEMD is that it is relatively easy to perform up to three computer experiments in one simulation. Basically, we conduct simultaneously a different one-dimensional experiment in each coordinate axis. This is shown in Figure 2, where the three $\mathbf{X}^\gamma$ are instead represented by corresponding physical analogues: concentration gradients and an electric field. If each experiment is operating in the linear transport regime, then it will not interfere with the others. Even if noticeable nonlinear effects are manifest, they may be corrected by a proper extrapolation of results to the low-field limit as demonstrated in the next section.

Using this technique permits up to a 3-fold increase in simulation efficiency. The three experiments, taken together, can generate up to $3(n - 1)$ independent pieces of information (fluxes). The regression procedure described above, in which ORR is not initially enforced, allows systems up to $n = 4$ to be fully resolved in one simulation. For $n = 3$, such as binary electrolytes, only two simultaneous experiments are required.

In the context of Evans and co-workers' color diffusion algorithm, our orthogonal-experiment algorithm amounts to assigning a *tensor* color charge to each molecule. (Recall that the color charge is the fictitious molecular property that couples to the external-field vector.) Under the action of a single external-field vector, such tensor color charges generate up to $n - 1$ independent species fluxes, in each of three coordinate directions.

4. Electrolyte Simulations

KCl and NaCl electrolyte simulations were performed using the same computer code, potential models, and simulation conditions described in paper 1.[1] At each concentration the equilibrium simulations were augmented by multiple NEMD simulations.

Nonlinear Transport. As discussed above, the imposition of strong external fields in the NEMD technique can lead to nonlinear behavior. In general, this requires that a series of NEMD simulations be performed, with an extrapolation to the zero-field limit. Figure 3 illustrates this extrapolation process. Shown are the NEMD and EMD (equilibrium molecular dynamics) results for the elements of the matrix $\mathbf{L}^0$, as well as least-squares fits of the NEMD data. The intercepts of the least-squares fits agree, within simulation uncertainties, with the EMD Green-Kubo results.

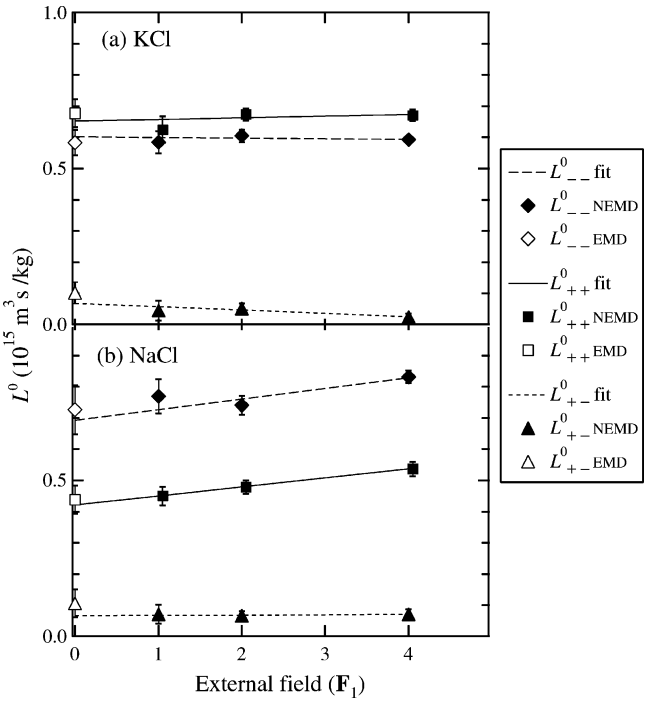

Figure 3. NEMD extrapolation compared to EMD results for 1 *m* KCl and NaCl. Basis field $\mathbf{F}_1$ is a 2-fold field acting on the ions.

The imposed fields in Figure 3 are multiples of a composite basis field, $\mathbf{F}_1$, which in one coordinate direction is an electric field of strength 10^8 V/m, and in another coordinate direction is a synthetic force of strength 10^8 eV/m driving salt diffusion through the solvent. The nonlinear behavior shown in Figure 3 is relatively small as given by the slopes of the fits. In this case, the use of a single NEMD simulation at field $\mathbf{F}_1$, rather than a zero-field extrapolation, is a computationally efficient option, since both lead to the same $\mathbf{L}^0$ within error limits. We performed each EMD simulation for three times as many time steps of each NEMD simulation. By comparing the resulting uncertainties in each calculation, it appears that NEMD is a more efficient technique than Green-Kubo EMD for obtaining bulk mass-transport coefficients.

In order for our NEMD results to be accurate, the simulation data must be collected only after a steady state for species fluxes has been reached, after turning on the external field. In the systems simulated here, any initial transients appear to be adequately damped within 10 ps. Nevertheless, NEMD data were collected only when 30 ps or greater had elapsed following the initiation of the external field. As an example, Figure 4 demonstrates the existence of a steady state during the simulation of 1 molar KCl operating under an electric field of 2×10^8 V/m. The cumulative averages of the species fluxes

$$\langle J(t) \rangle = \frac{1}{t}\int_0^t J \, d\tau \tag{10}$$

are given for the two ions. The cumulative averages in Figure 4 are generated from block averages taken over 10-ps intervals during the course of the simulation. Each block average can be considered an independent sample, because 10 ps is greater than the apparent decorrelation times for the respective fluxes, as indicated by Figure 6 in paper 1.

Figure 5 allows us to evaluate the degree to which the simultaneous NEMD experiments interfere with each other. In this case, we compare the calculated conductivities from NEMD electric-field simulations in which a concurrent salt-diffusion field is used ("2-fold NEMD") and in which no other field is used ("1-fold NEMD"). The departure of the 2-fold data from the 1-fold data shows that the two experiments interfere with each other or, in other words, exhibit nonlinear coupling. This interference is in addition to the nonlinearity observed in the 1-fold data. However, it is pleasing to see that all nonlinearities decrease as the fields are reduced and that the resulting NEMD zero-field extrapolations agree with each other and with the EMD results. Even if one were interested in conductivity only, the 2-fold simulations have a modest advantage over the 1-fold simulations in that transport information is extracted from two concurrent experiments, leading to lower uncertainties in conductivity for a given computational effort.

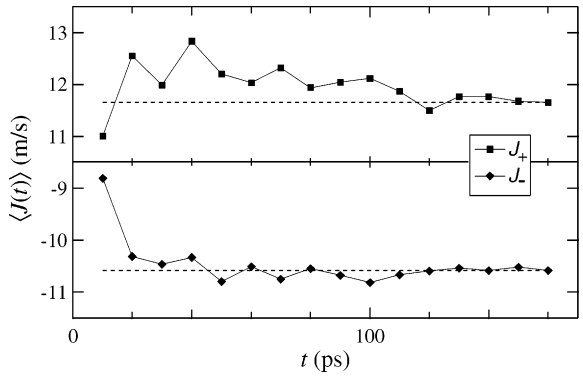

Figure 4. Cumulative averages of the ion fluxes for 1 molal KCl under an applied electric field of 2×10^8 V/m. The averages are given at 10-ps intervals. The lines serve as guides to the eye, with the final simulation averages being given by the dotted lines.

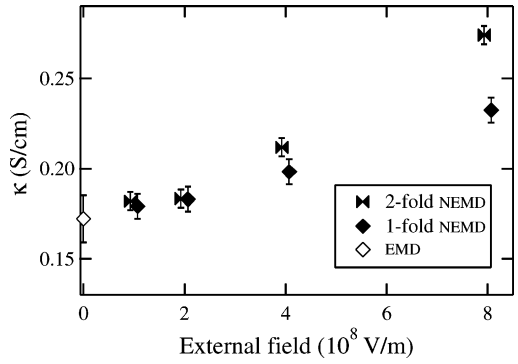

Figure 5. Nonlinearities in electrical conductivity with increasing field for 2 *m* KCl. 2-fold NEMD has a salt-diffusion-driving field orthogonal to the electric field; 1-fold NEMD has only the electric field. The 2-fold and 1-fold simulations were performed at the same field strengths; symbols have been offset horizontally for clarity.

A full presentation of the NEMD- and EMD-generated Stefan−Maxwell diffusivities is given in Figure 6. Figure 7 provides a comparison for electrical conductivity. In both figures, we see that the NEMD and EMD results are consistent. As discussed in paper 1, the agreement between simulation and experiment is semiquantitatively correct. We believe the largest source of difficulty is the overly strong association between the counterions. This acts to impede the motion of one ion relative to the other species in solution. The problem becomes more acute with increasing concentration, indicating that short-range, rather than long-range, interactions are suspect. We are not aware of any reliable and simple potential models of aqueous KCl and NaCl that overcome this strong-association problem, as indicated by reported mass-transport properties that are extremely sensitive to ion association. It is a nontrivial problem to faithfully reproduce the delicate balance of ion−ion and ion−solvent forces exhibited in real electrolytic solutions.

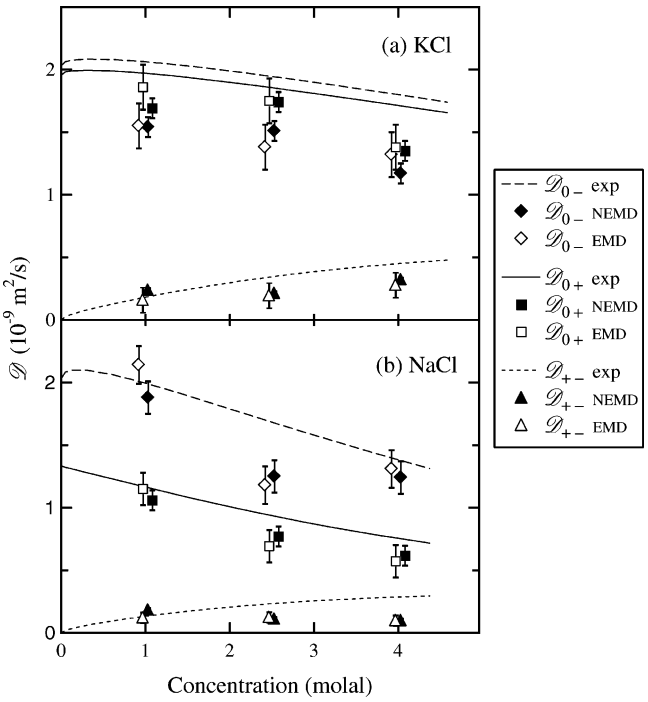

Figure 6. Simulated and experimental Stefan−Maxwell binary diffusivities for aqueous KCl and NaCl. Concentrations of 1, 2.5, and 4 *m* only were used; symbols have been offset horizontally for clarity. Some error bars are smaller in size than the symbols.

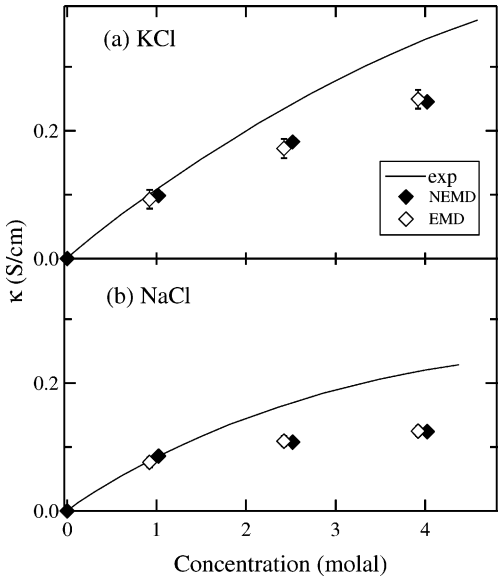

Figure 7. Simulated and experimental conductivities of aqueous KCl and NaCl. As in Figure 6, symbols have been offset for clarity. Some error bars are smaller in size than the symbols.

5. Conclusion

In this paper, we have demonstrated that the nonequilibrium and equilibrium (Green-Kubo) methods for simulating multicomponent diffusion generate nearly equal results, for simulations of binary electrolytic solutions. This provides evidence that both methods are measuring the same transport phenomena and that the unique assumptions made for each method are not debilitating. The agreement suggests that the truncation of the long-time tail at 10 ps does not introduce a large error in the Green-Kubo calculations and that the nonlinearities in the NEMD calculations are manageable. Nevertheless, we conclude that NEMD is generally a more computationally efficient simulation method than EMD.

This work provides a firm connection between molecular simulation and Stefan−Maxwell multicomponent diffusion. The limitations of the method are really the limitations of molecular dynamics itself. That is, if the relevant diffusional processes can be captured within the size and time scales accessible to MD, then all independent mass-transport coefficients can be calculated.

Acknowledgment. This work was supported by a National Science Foundation graduate fellowship and by the Assistant Secretary for Energy Efficiency and Renewable Energy, Office of Freedom CAR and Vehicle Technologies of the U.S. Department of Energy under Contract No. DE-AC03-76SF00098.

References and Notes

(1) Wheeler, D. R.; Newman, J. *J. Phys. Chem. B* **2004**, *108*, 18353−18361.
(2) Newman, J. *Electrochemical Systems*, 2nd ed.; Prentice Hall: Englewood Cliffs, NJ, 1991.
(3) Allen, M.; Tildesley, D. *Computer Simulation of Liquids*; Oxford Science: New York, 1989.
(4) MacElroy, J. *J. Chem. Phys.* **1994**, *101* (6), 5274.
(5) Heffelfinger, G. S.; Ford, D. M. *Mol. Phys.* **1998**, *94* (4), 659−671.
(6) Sunderrajan, S.; Hall, C. K.; Freeman, B. D. *J. Chem. Phys.* **1997**, *107* (24), 10714−10722.
(7) Thompson, A. P.; Ford, D. M.; Heffelfinger, G. S. *J. Chem. Phys.* **1998**, *109* (15), 6406−6415.
(8) Thompson, A. P.; Heffelfinger, G. S. *J. Chem. Phys.* **1999**, *110* (22), 10693−10706.
(9) Arya, G.; Chang, H.-C.; Maginn, E. J. *J. Chem. Phys.* **2001**, *115* (17), 8112−8124.
(10) Maginn, E. J.; Bell, A. T.; Theodorou, D. N. *J. Phys. Chem.* **1993**, *97*, 4173−4181.
(11) MacGowan, D.; Evans, D. J. *Phys. Rev. A* **1986**, *34* (3), 2133−2142.
(12) Evans, D.; Lynden-Bell, R.; Morriss, G. *Mol. Phys.* **1989**, *67*, 209.
(13) Evans, D. J.; Morriss, G. P. *Statistical Mechanics of Nonequilibrium Liquids*; Academic Press: London, 1990.
(14) Sarman, S.; Evans, D. J. *Phys. Rev. A* **1992**, *45* (4), 2370−2379.
(15) Müller-Plathe, F.; Rogers, S. C.; van Gunsteren, W. F. *J. Chem. Phys.* **1993**, *98* (12), 9895−9904.
(16) Hirschfelder, J.; Curtiss, C.; Bird, R. *Molecular Theory of Gases and Liquids*; Wiley: New York, 1954.
(17) Chandler, D. *Introduction to Modern Statistical Mechanics*; Oxford University Press: New York, 1987.
(18) van de Ven-Lucassen, I. M.; Vlugt, T. J.; van der Zanden, A. J.; Kerkhof, P. J. *Mol. Phys.* **1998**, *94* (3), 495−503.
(19) Nosé, S. *J. Chem. Phys.* **1984**, *81*, 511.
(20) Hoover, W. *Phys. Rev. A* **1985**, *31*, 1695.
(21) Evans, D.; Cui, S.; Hanley, H.; Straty, G. *Phys. Rev. A* **1992**, *46* (10), 6731−6734.
(22) Wien, M.; Malsch, J. *Ann. Physik* **1927**, *83*, 305.
(23) Szklarczyk, M.; Kainthla, R. C.; Bockris, J. O. *J. Electrochem. Soc.* **1989**, *136* (9), 2512−2521.